RSC Advances

PAPER

View Article Online
View Journal | View Issue

Cite this: *RSC Adv.*, 2021, **11**, 23355

SILP materials based on TiO_2–SiO_2 and TiO_2–SiO_2/lignin supports as new catalytic materials for hydrosilylation reaction – synthesis, physicochemical characterization and catalysis†

Olga Bartlewicz, *[ab] Mariusz Pietrowski, [a] Marta Kaczmarek[a] and Hieronim Maciejewski [ab]

The oxide system TiO_2–SiO_2 as well as a TiO_2–SiO_2/lignin system have been obtained by the sol–gel synthesis method and applied as supports in Supported Ionic Liquid Phase (SILP) materials. In total 24 SILP systems were obtained with ionic liquids containing imidazolium, pyridinium, phosphonium or sulfonic cations and bis(trifluoromethylsulfonyl)imide or methylsulfate anions, and homogeneous complexes of rhodium or platinum as the active phase. The supports and catalytic materials were subjected to thorough characterization by elemental analysis, XRD, SEM-EDX, IR, and TGA, and their particle size distribution and porous properties were assessed. The new SILP materials were used in hydrosilylation of 1-octene with 1,1,1,3,5,5,5-heptamethyltrisiloxane. The effectiveness of hydrosilylation reaction catalyzed by the obtained SILP materials for the polar and nonpolar reagents was assessed. All the catalytically active materials were proved to be easy to isolate and reuse, and the best SILP systems have been shown to be active in 10 or more subsequent catalytic cycles.

Received 21st May 2021
Accepted 25th June 2021

DOI: 10.1039/d1ra03966k

rsc.li/rsc-advances

Introduction

The reaction of hydrosilylation, permitting the addition of compounds containing the ≡Si–H group to compounds having multiple bonds, is an easy and effective method for obtaining organosilicon compounds. This reaction is commonly used not only in laboratory syntheses but also in large-scale industrial processes, including additive cross-linking of silicones, production of silane adhesion promotors and production of hybrid materials.[1–4] Recently, the hydrosilylation processes have been used for functionalization (introduction of functional groups) of different materials, for instance for production of organofunctional silicones (polydimethylsiloxanes), showing chemical reactivity, in contrast to the standard, chemically inert, silicones. Thanks to these properties it is possible to produce new hybrid materials showing unique properties depending on the type of functional group attached to the siloxane chain and maintaining the characteristic features of silicones, *i.e.* high elasticity and thermal stability.[2,5] The reaction of hydrosilylation is a catalytic process, usually taking place in the presence of homogeneous complexes of transition metals.[2,4] This fact generates problems related to the effective isolation of the catalyst from the post-reaction mixture. Sometimes it is even impossible to isolate the catalyst from the product, which is highly undesirable for economical (high cost of catalysts) and ecological (high toxicity of the metals used, even in trace amounts) reasons. That is why much attention is paid to heterogeneous catalytic systems for hydrosilylation reaction, that would permit easy isolation of the catalytically active substance from the post-reaction mixture and its use in subsequent catalytic cycles.[6–9] One of the recent solutions proposed for heterogenization of the homogeneous catalysts is based on the use of SILP (Supported Ionic Liquid Phase) materials. The SILP systems are obtained by physical impregnation of the support with an ionic liquid that immobilizes a given metal or metal complex. The stability and potential catalytic application of the SILP system depend on all its components.[10,11] The cost of SILP system production is much lower than that of liquid–liquid systems, mainly because of small amounts of the ionic liquid (10–20% wt relative to the support mass) and the active substance needed. Moreover, the SILP system can be easily isolated from the post-reaction mixture and used again in subsequent catalytic cycles, which also contributes to cost reduction. The use of a small amount of ionic liquid is also important because of the decreased risk of adsorption of contaminants and side products that can be formed in the process, which extends the time of the catalyst use.[11] SILP systems have been successfully used in many

[a]*Faculty of Chemistry, Adam Mickiewicz University in Poznań, Uniwersytetu Poznańskiego 8, Poznań, 61-614, Poland. E-mail: olga.bartlewicz@amu.edu.pl*

[b]*Adam Mickiewicz University Foundation, Poznań Science and Technology Park, Rubież 46, Poznań, 61-612, Poland*

† Electronic supplementary information (ESI) available. See DOI: 10.1039/d1ra03966k

chemical reactions, *e.g.* in the reactions of hydroformylation or the Heck and Suzuki processes.[12–14] The SILP systems based on silica support belong to the most often used catalytic materials of this type.[15] Recently, other supports have been used for production of SILP materials, *e.g.* zeolites, carbon nanotubes, resins or oxides.[16–18] From the group of the latter, particularly attractive seem to be the supports being combinations of at least two different oxides. Besides combining the unique properties of individual oxides, this solution permits enlargement of the surface area of the support. Such materials are most often obtained by the wasteless sol–gel method, which not only needs mild conditions, but also permits control of the morphology of the obtained support. Thanks to the processes of hydrolysis, condensation and removal of the solvent from the structure of the obtained alcogel, it is possible to get the oxide systems of high purity.[19,20] In our studies we applied this method for the synthesis of a hybrid oxide support composed of titanium dioxide and silica. The choice of these components was based on the idea of combining their particular properties. Titanium dioxide shows high chemical and thermal resistance, is non-toxic, biocompatible, has a high oxidizing potential and unique optical properties.[21–23] Silicon dioxide shows high mechanical strength and thermal resistance as well as large surface area.[24,25] The hitherto studies of TiO_2–SiO_2 have shown that this system is an excellent support in the processes of dye adsorption[26] and in catalytic processes.[27,28] Another interesting idea is a combination of inorganic–organic hybrids as catalysts supports. Attachment of lignin to the oxide strengthens the system and improves its sorption properties.[29] The structure of this biopolymer includes a number of functional groups, *e.g.* –OH, $-OCH_3$, C=O, which means that the material is able to easily link to other substances, including enzymes or metal complexes.[30]

In this paper we report the studies of new SILP materials obtained with the use of the oxide system TiO_2–SiO_2 and TiO_2–SiO_2/lignin as supports. These supports were subjected to impregnation with ionic liquids containing imidazolium, pyridinium, phosphonium or sulfonium cations or methylsulfate or bis(trifluoromethylsulfonyl)imide anions. Then the complexes of rhodium or platinum were immobilized on the supports surface. The obtained SILP systems were characterized as to their physicochemical and adsorption properties.

As our research group has many-year experience in catalysis of hydrosilylation processes,[31–33] this very reaction was used to test the catalytic activities of the new Rh-SILP and Pt-SILP systems and the possibilities of their isolation from post-reaction mixture and reuse. The reactions of hydrosilylation were performed with the use of polar and nonpolar olefins (1-octene, allyl-glycidyl ether, octafluoropentyl ether) and 1,1,1,3,5,5,5-heptamethyltrisiloxane, triethylsilane and triethoxysilane.

Experimental

Synthesis of titanium dioxide–silica support (TiO_2–SiO_2)

The synthesis of the inorganic oxide system TiO_2–SiO_2 was carried out by the sol–gel method with using tetraethoxysilane (TEOS) as silicon precursor and titanium(IV) isopropoxide (TIPP) as a titanium precursor.[26] Schematic synthesis reaction of TiO_2–SiO_2 is presented in Scheme 1 and the detailed procedure of synthesis is described in ESI.†

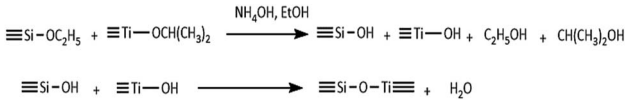

Scheme 1 The synthesis reaction of TiO_2–SiO_2 oxide system, obtained by sol–gel method.

Preparation of TiO_2–SiO_2/lignin support

○ **Modification of TiO_2–SiO_2 surface.** The TiO_2–SiO_2 surface was grafted by the dry method (Scheme 2) with the use of 3-(trimethoxysilyl)propyl isocyanate as a surface modifier.[34,35] Detailed description of the procedure can be found in ESI.†

○ **Synthesis of TiO_2–SiO_2/lignin material.** The two-stage process of obtaining TiO_2–SiO_2/lignin system was carried out according to the method reported in literature[35,36] and is briefly presented in Scheme 3. Detailed description of the procedure can be found in ESI.†

Preparation of Rh-SILP and Pt-SILP materials

SLIP materials were prepared using the method of physical impregnation. The earlier calcinated TiO_2–SiO_2 or TiO_2–SiO_2/lignin support (2 g) was impregnated with an ionic liquid (10% wt), which immobilized platinum (dichloro(1,5-cyclooctadiene) platinum(II)) or rhodium (Wilkinson's catalyst) catalyst (4×10^{-3}%),[35,37] as described in detail in ESI.†

Results and discussion

Physicochemical characterization of TiO_2–SiO_2 oxide system

By the sol–gel synthesis a series of TiO_2–SiO_2 oxide systems were obtained. In order to establish the effects of the composition of

Scheme 2 Process of modification of TiO_2–SiO_2 surface.

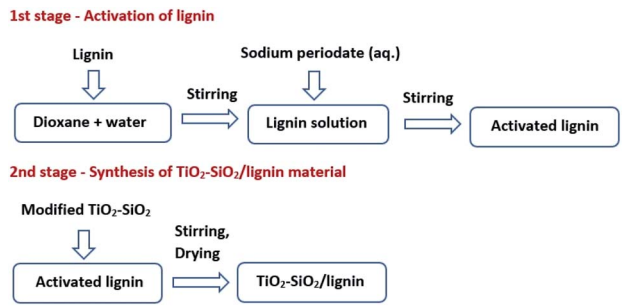

Scheme 3 Synthesis of TiO_2–SiO_2/lignin material.

Table 1 Thermal stability of obtained inorganic oxide supports

Sample	T_{onset}[a] [°C]	5% weight loss [°C]
SiO2	179.40	985[b] (1.22%)
TiO2	254.15	847.62
TiO_2–SiO_2 (0.75 : 0.25)	205.85	271.84
TiO_2–SiO_2 (0.50 : 0.50)	223.21	210.71
TiO_2–SiO_2 (0.25 : 0.75)	248.01	197.73

[a] Onset decomposition temperature. [b] Percentage weight loss less than 5%.

the oxide systems on their adsorption properties, the precursors of silicon and titanium were used at different molar ratios of 0.75 (TEOS) : 0.25 (TIPP), 0.50 (TEOS) : 0.50 (TIPP) and 0.25 (TEOS) : 0.75 (TIPP). The porous properties of the obtained oxide systems were compared with those of the individual oxides being components of the TiO_2–SiO_2 system, obtained by the same method, see Table S2 (ESI).† The results confirmed the influence of different proportions of silicon and titanium precursors on the porous properties of the TiO_2–SiO_2 systems obtained. With increasing molar concentration of TEOS, the surface area as well as the pore volume and average pore diameter of the support increase. The adsorption parameters of all TiO_2–SiO_2 systems obtained were better than those of the individual components of the system (silica dioxide and titanium dioxide). The largest surface area was obtained for the TiO_2–SiO_2 system synthesized with the highest molar ratio of TEOS, while the smallest surface area was found for the system synthesized with the greater amount of TIPP. The molar ratio of silicon and titanium precursors also affected the thermal stability of the oxide systems obtained. As follows from the results of thermogravimetric measurements (TG), a greater amount of tetraethoxysilane used for the synthesis results in a higher thermal resistance of the oxide system, Table 1. Unfortunately, the thermal stabilities of the TiO_2–SiO_2 systems although satisfactory, were not as high as the stabilities of the individual oxides TiO_2 and SiO_2.

From among the obtained TiO_2–SiO_2 systems, the one characterized with the largest surface area of 328 $m^2\ g^{-1}$ (Table S2 (ESI)†) was chosen for further studies. This system was synthesized using TEOS and TIPP at the molar ratio of 0.75 : 0.25. The effectiveness of the catalytic process significantly depends on the appropriate preparation of the support surface for adsorption. At first the support was subjected to calcination to eliminate the physically adsorbed water and contaminants introduced at the stage of synthesis. The calcination of TiO_2–SiO_2 resulted in a decrease in its surface area (Table 2), which indicates a high contribution of micropores in the TiO_2–SiO_2 structure prior to this process, which may limit the effectiveness of adsorption. In the process of calcination the micropores join one another to form mesopores, which is confirmed by the increase in the pore diameter in the support after the process, Table 2.

The temperature of calcination determines the formation of particular crystalline forms in the support structure. When it is above 600 °C, the TiO_2–SiO_2 support is composed of anatase and rutile, with significant prevalence of the latter. According to literature data, rutile shows poorer adsorption properties than anatase as the latter has large surface area and high degree of the surface hydroxylation. A too high temperature of calcination leads to pore sintering and formation of agglomerates.[38,39] In view of the above, the temperature of 600 °C was chosen as the optimum.

XRD diffractogram (Fig. 1) of the mixed oxide support after calcination revealed its amorphous structure, which is reflected in its large surface area. The intensive bands corresponding to amorphous silica overlap the bands assigned to the crystalline structure of titanium dioxide (Fig. 1.). The XRD patterns of SiO_2 and TiO_2 oxides are presented in Fig. S15 in ESI.†

Determination of the particle size distribution, shown in Fig. 2, proved that for TiO_2–SiO_2 (TS) system it is monomodal in the range 122–396 nm. The largest volume contribution bring the particles of 220 nm (33%) and 255 nm (32%) diameters. The support obtained in the synthesis with the use of precursors of the two oxides was found to have smaller size particles than the individual oxides SiO_2 and TiO_2, but poorer homogeneity. Titanium dioxide and silica have bimodal particle size distributions, while the system of TiO_2–SiO_2 and lignin (TS_L) has a trimodal one. The latter system was also characterized by a high polydispersity coefficient (0.868) indicating its great inhomogeneity. Moreover, the incorporation of lignin to the oxide system TiO_2–SiO_2 resulted in enlargement of the particle size of the system, the dominant particles in TS_L have the mean diameter of 1313 nm.

To confirm the composition of the systems studied, they were subjected to energy-dispersive X-ray microanalysis (EDX), Table 3, which confirmed the presence of titanium dioxide and silica in the structures of TS and TS_L. These two supports showed high contents of silicon, titanium and oxygen, while the

Table 2 The adsorption properties of the obtained TiO_2–SiO_2 support before and after the calcination process (CP)

Inorganic support	BET surface area [$m^2\ g^{-1}$]	Total pore volume [$cm^3\ g^{-1}$]	Average pore diameter [nm]
Before CP	464	0.93	7.97
After CP	328	0.91	10.95

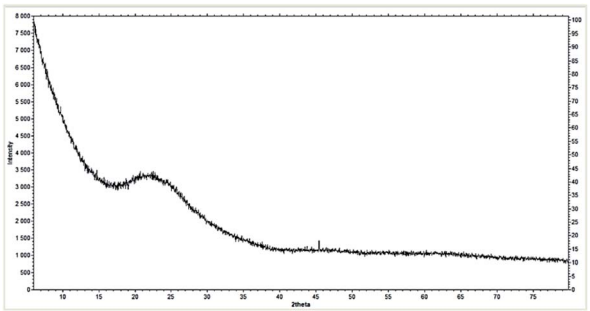

Fig. 1 XRD diffractogram of inorganic support TiO_2–SiO_2.

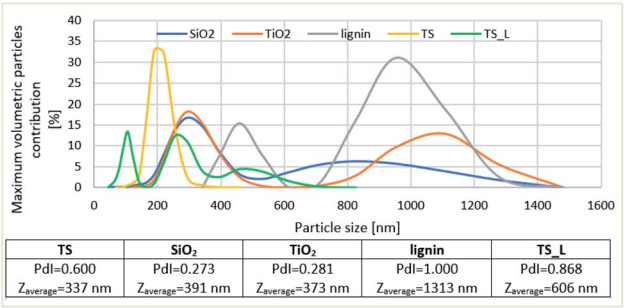

TS	SiO_2	TiO_2	lignin	TS_L
PdI=0.600	PdI=0.273	PdI=0.281	PdI=1.000	PdI=0.868
$Z_{average}$=337 nm	$Z_{average}$=391 nm	$Z_{average}$=373 nm	$Z_{average}$=1313 nm	$Z_{average}$=606 nm

Fig. 2 Distribution of particles size and maximum volumetric particles contribution in the selected supports.

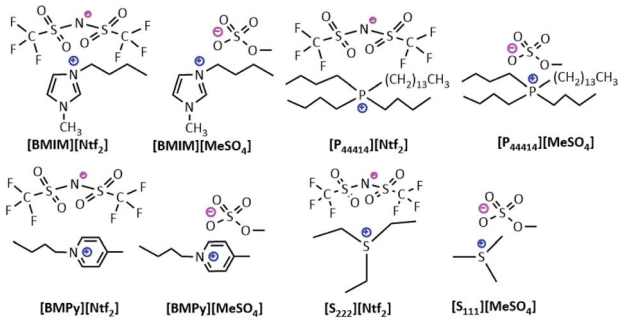

Fig. 3 Ionic liquids applied in the presented study.

TS_L apart from these elements had a high content of carbon and trace amounts of sulfur.

Preparation of SILP materials

The aim of the study was to evaluate the impact of the support structure as well as the type of the ionic liquid making the SILP system, on its stability and catalytic performance. The analysis was performed for eight ionic liquids containing imidazolium, pyridinium, phosphonic or sulfonic cations and methylsulfate and bis(trifluoromethylsulfonyl)imide anions, Fig. 3. The methods of syntheses of the ionic liquids, their spectroscopic and thermogravimetric characterization are given in ESI.†

Another important parameter of the Supported Ionic Liquid Phase systems is the amount of the ionic liquid, its excess may hinder the assess of products to the catalyst surface, while a too small amount of the liquid leads to poor impregnation of the support surface and faster leaching of the immobilized catalytically active phase. In order to determine the optimum amount of the liquid, a series of the SILP systems containing 10%, 15% or 20% wt of $[P_{44414}][Ntf_2]$ were obtained and subjected to catalytic tests, Table S8.† For the systems containing the platinum complex as the active phase, the catalytic activity was at the same level for the samples with 10% and 15% content of ionic liquid, but for the ionic liquid content of 20%, the reaction efficiency was significantly lower. For the samples with the rhodium complex as the active phase, the highest yield was obtained for the ionic liquid content of 10% wt, while it was lower for the systems with 15% and 20% wt of IL. In view of the fact that the improvement in catalytic activity with increasing content of ionic liquid was rather insignificant and taking into account the economic reasons, the further studies were performed for the SILP samples with 10% wt of an ionic liquid relative to the mass of the support. As a result of physical impregnation of the supports TiO_2–SiO_2 and TiO_2–SiO_2/lignin with the above mentioned ionic liquids and immobilization of the platinum or rhodium complexes, a series of 24 new SILP materials was obtained. For the sake of comparison 4 SILP systems with sulfonic ionic liquids supported on silica were prepared, Table 4.

Table 3 EDX analysis of obtained TiO_2–SiO_2 and TiO_2–SiO_2/lignin supports

	Element content [wt%]					
Support	C	O	Na	Si	Ti	S
TS	2.08	47.51	—	30.89	19.50	—
TS_L	9.74	46.57	1.04	26.49	16.09	0.2

Physicochemical characterization of the obtained SILP materials

Characterization of adsorption properties. All the obtained SILP systems were subjected to the studies aimed at

Table 4 SILP materials with TiO_2–SiO_2 and TiO_2–SiO_2/lignin supports

Support	Ionic liquid	Catalyst	Sample name
TiO_2–SiO_2	—	—	TS
	$[BMIM][Ntf_2]$	$Rh(PPh_3)_3Cl$	TS_1.1_Rh
		$Pt(cod)Cl_2$	TS_1.1_Pt
	$[BMPy][Ntf_2]$	$Rh(PPh_3)_3Cl$	TS_2.1_Rh
		$Pt(cod)Cl_2$	TS_2.1_Pt
	$[P_{44414}][Ntf_2]$	$Rh(PPh_3)_3Cl$	TS_3.1_Rh
		$Pt(cod)Cl_2$	TS_3.1_Pt
	$[S_{222}][Ntf_2]$	$Rh(PPh_3)_3Cl$	TS_4.1_Rh
		$Pt(cod)Cl_2$	TS_4.1_Pt
	$[BMIM][MeSO_4]$	$Rh(PPh_3)_3Cl$	TS_1.2_Rh
		$Pt(cod)Cl_2$	TS_1.2_Pt
	$[BMPy][MeSO_4]$	$Rh(PPh_3)_3Cl$	TS_2.2_Rh
		$Pt(cod)Cl_2$	TS_2.2_Pt
	$[P_{44414}][MeSO_4]$	$Rh(PPh_3)_3Cl$	TS_3.2_Rh
		$Pt(cod)Cl_2$	TS_3.2_Pt
	$[S_{111}][MeSO_4]$	$Rh(PPh_3)_3Cl$	TS_4.2_Rh
		$Pt(cod)Cl_2$	TS_4.2_Pt
TiO_2–SiO_2_ lignin	—	—	TS_L
	$[P_{44414}][Ntf_2]$	$Rh(PPh_3)_3Cl$	TS_L_3.1_Rh
		$Pt(cod)Cl_2$	TS_L_3.1_Pt
	$[S_{222}][Ntf_2]$	$Rh(PPh_3)_3Cl$	TS_L_4.1_Rh
		$Pt(cod)Cl_2$	TS_L_4.1_Pt
	$[P_{44414}][MeSO_4]$	$Rh(PPh_3)_3Cl$	TS_L_3.2_Rh
		$Pt(cod)Cl_2$	TS_L_3.2_Pt
	$[S_{111}][MeSO_4]$	$Rh(PPh_3)_3Cl$	TS_L_4.2_Rh
		$Pt(cod)Cl_2$	TS_L_4.2_Pt
SiO_2	$[S_{222}][Ntf_2]$	$Rh(PPh_3)_3Cl$	S_4.1_Rh
		$Pt(cod)Cl_2$	S_4.1_Pt
	$[S_{111}][MeSO_4]$	$Rh(PPh_3)_3Cl$	S_4.2_Rh
		$Pt(cod)Cl_2$	S_4.2_Pt

characterization of their porosity. Results of BET analysis permitted assessment of the effect of ionic liquid adsorption on the specific surface area, total pore volume and average diameter of the particles in the systems. Determination of the adsorption parameters confirmed the effectiveness of the process of IL adsorption on the surface of TiO_2–SiO_2 and TiO_2–SiO_2/lignin, as proved by a considerable decrease in the surface area of SILP systems in comparison to that of the corresponding supports. The adsorbed ionic liquid penetrates the pores leading to a significant decrease in their volume and an increase in their diameters. The parameter describing the degree of pore filling (α), whose values for the SILP materials studied varied in the range 0.11–0.29, indicated that the pores of the supports were not filled up, however, its value of over 0.20 for some samples means that a large number of pores in the support are blocked. The surface of SILP materials after the adsorption of ionic liquids is also characterized by the thickness of the ionic liquid layer adsorbed. For the obtained SILP materials the adsorbed layer thickness varied in the range 0.57–0.72 nm for TiO_2–SiO_2 systems and 0.46–0.72 nm for the TiO_2–SiO_2/lignin systems. To characterize the porous structures of the systems obtained measurements of nitrogen sorption were performed at 77 K, see Table 5. The isotherms of nitrogen sorption, presented in Fig. S17,† correspond to the structure of mesoporous materials, according to IUPAC classification.[40] The adsorption parameters characterizing all obtained SILP systems are collected in Table S4 in the ESI.†

Textural properties. The effectiveness of ionic liquids adsorption on the surfaces of the support systems TiO_2–SiO_2 and TiO_2–SiO_2/lignin was evidenced by results of measurements by IR, SEM-EDX, TG methods, elemental analysis and particle size distribution determination. The IR spectra of Rh-SILP and Pt-SILP systems showed the bands characteristic of particular ionic liquids, Fig. S18–S29, ESI.† The bands assigned to alkyl groups, present in the spectra of all ionic liquids used, appeared in the range 2961–2880 cm^{-1}. For the sample with phosphonic ionic liquid, the characteristic and very intensive band corresponding to the P–CH_2–, appeared at about 2926 cm^{-1}. The increased percentage content of carbon, fluor or sulfur, observed in the results of SEM-EDX analysis, confirmed the presence of adsorbed ionic liquids containing methylsulfate and bis(trifluoromethylsulfonyl)imide anions, Table 6. The SILP systems with the ionic liquid with phosphonium cation ([P_{44414}][Ntf_2] and [P_{44414}][$MeSO_4$]) were found to contain phosphorus in the amount of 0.52–0.61%. The concentration of the platinum and rhodium complexes used as the active phase in the SILP systems was below the detection level of the SEM-EDX analyzer. In order to confirm the effectiveness of the immobilization of these complexes, special SILP samples with thirty times higher concentrations of the Wilkinson catalyst and dichloro(1,5-cyclooctadien)platinum(II) complex. Results of the analysis, presented in Table S5, ESI,† revealed the presence of 0.25% of rhodium and 0.29% of platinum.

Results of the elemental analysis of selected SILP systems revealed increased percentage contents of N, C, H and S relative

Table 6 SEM-EDX analysis of selected SILP materials and supports

	Element content [wt%]						
Sample	C	O	F	Si	S	Ti	P
TS	2.1	47.5	—	30.8	—	19.5	—
TS_L	9.7	46.5	—	26.4	0.2	16.1	—
TS_1.1_Rh	2.6	42.8	1.4	31.4	0.9	20.5	—
TS_2.1_Rh	3.6	43.6	1.5	30.4	0.9	19.6	—
TS_3.1_Rh	6.2	44.8	1.4	28.9	0.7	16.9	0.5
TS_L_3.1_Rh	15.3	43.2	1.4	22.4	1.2	14.4	0.6
TS_4.1_Rh	5.2	42.2	1.8	28.0	2.2	20.2	—
TS_L_4.1_Rh	11.9	40.3	4.3	22.5	3.2	16.5	—
TS_1.2_Rh	4.2	46.0	—	28.9	1.3	19.5	—
TS_2.2_Rh	4.7	45.9	—	27.3	1.1	20.7	—
TS_3.2_Rh	5.0	45.9	—	27.9	1.2	18.9	0.5
TS_L_3.2_Rh	13.1	43.2	—	26.5	0.7	14.7	0.5
TS_4.2_Rh	4.2	46.6	—	27.7	2.2	19.0	—
TS_L_4.2_Rh	12.9	44.7	—	22.7	3.0	14.8	—

Table 5 Adsorption characteristic of obtained SILP materials

Sample	BET surface area [m^2 g^{-1}]	Total pore volume [cm^3 g^{-1}]	Average pore diameter [nm]	α^a	Layer thickness^b [nm]
TS	328	0.91	10.95	—	—
TS_L	176	0.51	11.43	—	—
TS_1.1_Pt	214	0.65	11.93	0.28	0.65
TS_2.1_Pt	204	0.69	11.25	0.24	0.62
TS_3.1_Pt	189	0.69	12.36	0.24	0.57
TS_4.1_Pt	210	0.69	11.38	0.24	0.64
TS_L_3.1_Pt	82	0.36	13.71	0.29	0.46
TS_L_4.1_Pt	90	0.38	13.43	0.25	0.51
TS_1.2_Pt	224	0.66	11.21	0.27	0.68
TS_2.2_Pt	241	0.69	10.95	0.20	0.70
TS_3.2_Pt	222	0.67	10.26	0.23	0.65
TS_4.2_Pt	246	0.72	10.37	0.18	0.72
TS_L_3.2_Pt	106	0.41	13.95	0.19	0.60
TS_L_4.2_Pt	127	0.45	12.22	0.11	0.72

[a] Pore filling degree of support as the ratio IL volume/support pore volume. [b] Ratio of the IL volume used for coating and the initial surface area.

to those in pure supports. This result is an additional evidence of the presence of an ionic liquid on the surface of TiO_2–SiO_2 and TiO_2–SiO_2/lignin supports. On the basis of the percentage contents of carbon in the SILP samples studied it was possible to estimate the degree of the supports coverage with the ionic liquid, using the Berendsen formula.[41] The surface coverage was 1.54 μmol m^{-2} for TS_4.1_Pt, 2.12 μmol m^{-2} for TS_4.2_Pt and 1.51 μmol m^{-2} for TS_L_4.1_Pt. The results of elemental analysis are displayed in Table S6 in the ESI.† Comparisons of SEM images of the support before and after the impregnation with an ionic liquid and rhodium complex impregnation revealed changes in the number of agglomerates in the systems structures, Fig. 4. After the adsorption of ionic liquid the sample structure is more homogeneous and the agglomerates are much smaller than in pure supports. It is not only a consequence of impregnation but also of the process of SILP materials preparation. As a result of vigorous stirring of the support in the solution containing the ionic liquid and a given metal complex, the TiO_2–SiO_2 particles were broken and divided into smaller ones, which reduced the number and size of the agglomerates. The SILP surface is also appreciably smoothened relative to that of the pure support, which is attributed to the presence of the ionic liquid inside the pores of TiO_2–SiO_2 support.

The mean diameter of the nanoparticles was observed to decrease after the ionic liquid adsorption. Moreover, as follows from the data presented in Table S7,† the process of adsorption resulted in deterioration of the sample homogeneity, manifested by an increase in the polydispersity index (PdI) for TS_4.1_Pt and TS_L_4.1._Pt. According to the results of thermogravimetric (TG) measurements, the SILP systems containing ionic liquids with imidazolium, pyridinium and phosphonium cations are stable above 300 °C, irrespective of the anion used. Interestingly, for the SILP systems with sulfonic ionic liquids, the type of anion had an impact on their thermal stability, the systems with $[S_{222}][Ntf_2]$ were stable up to about 270 °C, while those with $[S_{111}][MeSO_4]$, were stable up to 200 °C. The incorporation of lignin to TiO_2–SiO_2 also resulted in deterioration of thermal stability. However, all SILP materials were thermally stable at 100 °C, at which hydrosilylation was performed. Results of TG analysis are shown in Table S3 (ESI).†

Catalytic activity. The catalytic activity of the obtained SILP materials was tested in the hydrosilylation of 1-octene with 1,1,1,3,5,5,5-heptamethyltrisiloxane (HMTS) with the reagents ratio of 1 : 1, and the amount of rhodium or platinum was of

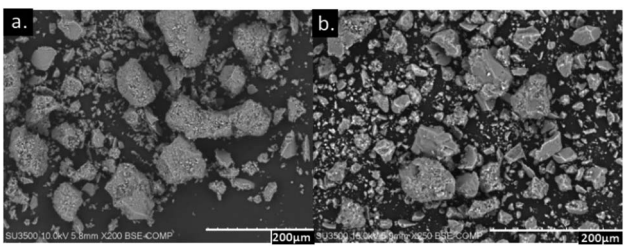

Fig. 4 The structure of TiO_2–SiO_2 before (a) and after (b) physical impregnation of $[P_{44414}][Ntf_2]$ and rhodium catalyst on its surface.

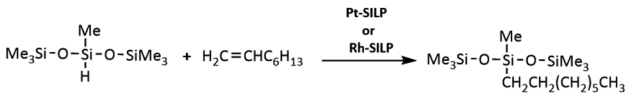

Scheme 4 Hydrosilylation of 1-octene with HMTS, catalyzed by Rh-SILP and Pt-SILP materials.

10^{-5} mol per 1 mol Si–H. The reaction was selective, leading only to the anti-Markovnikov β-addition product, Scheme 4.

At the next step, the optimum concentrations of the rhodium and platinum complexes were chosen. The use of the complexes at 10^{-4} mol was found to shorten the reaction to 20 minutes with no significant effect on the reaction efficiency. When the complexes were used at the concentration of 10^{-6} mol, the yield was lowered to 30% and the reaction time was extended to over 1 hour. The best results were obtained for the systems with the active complexes concentration of 10^{-5} mol of Rh or Pt per mol Si–H. The yields of the reactions catalyzed with the SILP materials obtained in six subsequent catalytic cycles are presented in Tables 7 and 8. The best SILP systems were active much longer, which is evidenced by the TON and TOF coefficients given in Table 9. The methodology of catalytic tests is described in detail in the ESI.†

According to the yields obtained, all the SILP systems were active in the test hydrosilylation reaction. A significant difference in yield was noted between the SILP with $[Ntf_2]^-$ and that with $[MeSO_4]^-$ anion, the yield of the former was much higher and they were catalytically active much longer that the systems with $[MeSO_4]^-$. The difference was particularly pronounced for the systems with the rhodium complex, as indicated by the values of TON and TOF. For the samples with $[Ntf_2]^-$ anion, such as: TS_1.1_Rh and TS_2.1_Rh, the value of TON were 304 000 and 706 000 and TOF were 0.61×10^6 and 1.41×10^6 h^{-1}, respectively. The samples with $[MeSO_4]^-$ anion – TS_1.2_Rh and TS_2.2 were characterized by lower values of TON and TOF coefficients of 166 000 and 134 000 (TON) and 0.33 and 0.27×10^6 h^{-1} (TOF), respectively. It should be mentioned that the systems of SILP with the ionic liquids containing aromatic cations are considered less effective

Table 7 Yield of product in 6 subsequent catalytic cycles of hydrosilylation reaction of 1-octene with HMTS catalyzed by SILP materials with $[Ntf_2]^-$ anion

Catalytic cycle no.	TS_1.1_Rh	TS_1.1_Pt	TS_2.1_Rh	TS_2.1_Pt	TS_3.1_Rh	TS_3.1_Pt	TS_4.1_Rh	TS_4.1_Pt
1	99	99	99	99	99	99	99	99
2	99	99	99	99	99	99	99	99
3	53	99	99	99	88	99	70	99
4	19	99	99	99	86	99	50	99
5	19	99	80	88	73	99	50	99
6	10	62	80	53	42	63	50	99
	99–50%			49–30%		29–0%		

Table 8 Yield of product in 6 subsequent catalytic cycles of hydrosilylation reaction of 1-octene with HMTS catalyzed by SILP materials with $[MeSO_4]^-$ anion

Catalytic cycle no.	TS_1.2_Rh	TS_1.2_Pt	TS_2.2_Rh	TS_2.2_Pt	TS_3.2_Rh	TS_3.2_Pt	TS_4.2_Rh	TS_4.2_Pt
1	90	99	82	99	99	99	64	99
2	42	66	35	99	79	99	56	99
3	18	28	17	99	67	99	52	99
4	16	13	—	88	59	81	37	99
5	—	—	—	78	59	71	37	99
6	—	—	—	77	58	70	16	99
	99–50%			49–30%			29–0%	

because of the electrostatic interactions in the ring strongly binding the cation and the anion, which hinders the access of substrates to the immobilized catalyst.[42,43] This phenomenon does not take place in the branched ionic liquids, *i.e.* phosphonium and sulfonic ones. The SILP systems with the two latter liquids show very good catalytic performance, irrespective of the type of anion. The systems with platinum complexes show greater stability and higher catalytic activity. It may be a consequence of the stronger ionic character of Pt (II) in $[Pt(cod)Cl_2]$ than Rh(I) in the Wilkinson catalyst. Thus, the platinum catalyst enters into stronger interactions with ionic liquids, endowing the catalyst with higher stability and better catalytic performance. For the platinum catalysts, the best results were obtained for the systems with TiO_2–SiO_2 as a support and sulfonic ionic liquid (TS_4.1_Pt and TS_4.2_Pt), that were active even in 15 subsequent catalytic cycles. From among the SILP systems with the rhodium complex, the best catalytic performance was noted for TS_2.1_Rh.

The catalytic performance of the SILP materials based on TiO_2–SiO_2 support were compared with the results obtained for the systems based on mesoporous silica. In the tests we used *Davisil grade 62* silica of the surface area of 302 $m^2\ g^{-1}$, pore volume of 1.14 $cm^3\ g^{-1}$ and average pore diameter of 11.39 nm. The silica surface was impregnated with sulfonic liquid with $[Ntf_2]^-$ or $[MeSO_4]^-$ anions and then the platinum $[Pt(cod)Cl_2]$ or rhodium $[Rh(PPh_3)_3Cl]$ complexes were immobilized on the silica. As follows from the results of catalytic tests presented in Table S9, ESI,† the yield of the hydrosilylation reaction was much lower than when using the corresponding SILP systems supported on TiO_2–SiO_2. For the systems Rh-SILP significant differences were observed in the system's stability in subsequent catalytic cycles. For the systems S_4.1_Rh and S_4.2_Rh, already in the second catalytic cycle the yield of the reaction decreased by more than half and in subsequent cycles – to 20–30% or to zero. For the systems with platinum and silica support, the decrease in catalytic activity and stability was also faster than for the corresponding systems supported on TiO_2–SiO_2. The TON and TOF values for the most active system based on SiO_2 were 585 000 and $1.17 \times 10^6\ h^{-1}$, respectively, while for the most active system supported on TiO_2–SiO_2 the TON and TOF vales were 1 302 000 and $2.60 \times 10^6\ h^{-1}$, respectively. An important result was determination of the profiles of hydrosilylation reaction catalyzed by the tested catalysts. The profiles were obtained for TS_4.1_Pt and TS_2.1_Rh, as the reactions in the presence of these catalysts were characterized by high yields. The catalytic activities of the SILP systems obtained were compared with those of the precursors of the catalysts, *i.e.* $[Pt(cod)Cl_2]$ and $[Rh(PPh_3)_3Cl]$, used for their preparation, and the results are presented in Fig. 5. In the FT-IR *in situ* analysis, the decay of the band assigned to the ≡Si–H bond in the HMTS molecule at 913 cm^{-1} was monitored. The reaction profiles were determined on the basis of the ≡Si–H conversion expressed as the change in the area of the monitored band. The SILP materials studied were found to lead to full Si–H conversion in a time shorter than 30 minutes, while the system TS_2.1_Rh was characterized by a much longer time of activation, close to 27 minutes, than the homogeneous rhodium catalyst. The reaction profiles obtained for the two catalysts are much different. In the presence of the Wilkinson catalyst after a nine-minute activation, the Si–H conversion rapidly increased up to almost 100%

Table 9 TON and TOF coefficients for SILP materials in hydrosilylation reaction

SILP material	TON	TOF, $\times 10^6\ h^{-1}$
TS_1.1_Rh	304 000	0.61
TS_1.1_Pt	792 000	1.58
TS_2.1_Rh	706 000	1.41
TS_2.1_Pt	682 000	1.36
TS_3.1_Rh	639 000	1.28
TS_3.1_Pt	668 000	1.34
TS_4.1_Rh	534 000	1.07
TS_4.1_Pt	1 302 000	2.60
TS_1.2_Rh	166 000	0.33
TS_1.2_Pt	206 000	0.21
TS_2.2_Rh	134 000	0.27
TS_2.2_Pt	802 000	1.60
TS_3.2_Rh	616 000	1.23
TS_3.2_Pt	809 000	1.62
TS_4.2_Rh	262 000	0.52
TS_4.2_Pt	1 140 000	2.28

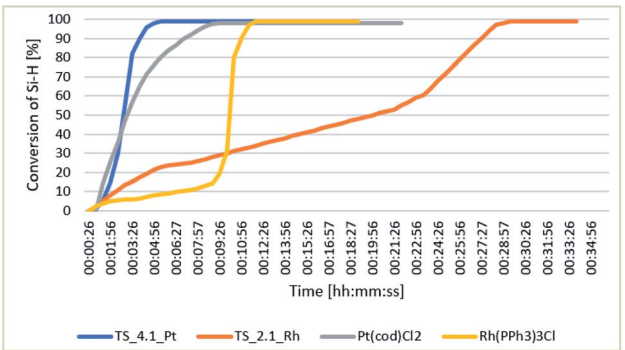

Fig. 5 Changes in the conversion of Si–H as a function of time for the hydrosilylation of 1-octene with HMTS, catalyzed by SILP materials with rhodium and platinum complexes.

Table 10 Yield of hydrosilylation reaction catalyzed by SILP materials supported on TiO_2–SiO_2/lignin

Catalytic cycle no.	TS_L_3.1_Rh	TS_L_3.1_Pt	TS_L_4.1_Rh	TS_L_4.1_Pt	TS_L_3.2_Rh	TS_L_3.2_Pt	TS_L_4.2_Rh	TS_L_4.2_Pt
1	26	35	31	56	35	50	0	33
2	26	30	28	47	27	31	—	15
3	21	29	20	41	15	25	—	0
4	0	0	0	42	0	10	—	—
TON	73 000	94 000	79 000	252 000	77 000	116 000	0	48 000
TOF $\times 10^6$ h^{-1}	0.15	0.19	0.16	0.50	0.15	0.23	0	0.96
99–50%		49–30%			29–0%			

conversion in 10 minutes. In the presence of the rhodium catalyst, the process of activation started in the second minute of the reaction and lasted till the 22nd minute and then the Si–H conversion fast increased reaching almost 100%. The reaction profiles in the presence of a platinum homogeneous catalyst and the Pt-SILP system are very similar. The Pt-SILP system needed a little longer time of activation than $[Pt(cod)Cl_2]$, however, the time needed for full Si–H conversion was by 3 minutes shorter. The process of hydrosilylation in the presence of each of the platinum catalysts was fast and with high conversion.

Another SILP system studied was supported on a hybrid, inorganic–organic material composed of TiO_2–SiO_2 and lignin and contained phosphonium and sulfonic ionic liquids and the earlier used homogeneous platinum and rhodium catalysts. The catalytic materials were used in the hydrosilylation of 1-octene with HMTS, the results are presented in Table 10. The SILP materials supported on TiO_2–SiO_2/lignin were characterized by low catalytic activity. Almost for all such SILP materials the reaction yield was below 30%. The extension of reaction time to one hour did not improve the yield. The best catalytic performance was obtained for the SILP system with ionic liquid containing $[Ntf_2]^-$. Low catalytic activity may be a result of the decreased surface area and pore volume in TiO_2–SiO_2/lignin than for the support without lignin. The changes also affected the effectiveness of the ionic liquids adsorption on the support surface and further immobilization of a metal complex, consequently, the obtained SILP systems with lignin showed poor stability and poor leaching resistance.

For the SILP systems showing the best catalytic performance: TS_4.1_Pt, TS_4.2_Pt and TS_2.1_Rh, the effects of different reagents on the product yield were evaluated. The reactions were run for polar and nonpolar olefins: 1-octene, allyl-glycidyl ether, octafluoropentyl ether, and the silicon compounds: HMTS, triethylsilane and triethoxysilane (TriEOS). The results are collected in Table 11 and imply that Pt-SILP materials show higher catalytic activity in the first cycle, in almost all hydrosilylation reactions tested, irrespective of the type of reagents used. For all SILP systems studied the attempts were made to isolate them from the post-reaction mixture and reuse in subsequent cycles, but in most cases the materials were inactive or their catalytic activity rapidly decreased after the second or the third catalytic cycle. The reactions with allyl-glycidyl ether and octafluoropentyl ether catalyzed by Pt-SILP were characterized by very high yield, but when Rh-SILP was used, their yield was very low. Irrespective of the type of SILP catalytic system, the efficiency of the reaction of olefin hydrosilylation with triethylsilane was very low. The use of triethoxysilane (TriEOS) resulted in the increase in the yield of the reactions with all olefins. The best results were obtained for the reaction of TriEOS with 1-octene in the presence of Pt-SILP materials, not only a high yield was obtained, but the Pt-SILP systems maintained activity in subsequent catalytic cycles. Slightly worse results were obtained in the reaction of hydrosilylation between TriEOS and the ethers. The catalytic activity of SILP TS_2.1_Rh was found much lower than the activities of the systems containing platinum. The best catalytic results were obtained for the systems with HMTS and TriEOS, containing electron-withdrawing substituents, and nonpolar olefin (1-octene). For these systems, in the presence of Pt-SILP catalysts, not only high yields were obtained, but also the catalytically active phase was

Table 11 Yield of hydrosilylation reaction with different reagents, catalyzed by the best SILP materials supported on TiO_2–SiO_2

Si–H	$H_2C{=}CHCH_2$-R, where -R:	Yield of the reaction [%] TS_4.1_Pt	TS_2.1_Rh	TS_4.2_Pt
HMTS	$-C_5H_{11}$	99	99	99
	TON	1 302 000	1 140 000	706 000
	TOF $\times 10^6$ h^{-1}	2.60	2.28	1.41
	$-OCH_2CHOCH_2$	86	7	85
	TON	38 000	—	330 000
	TOF $\times 10^6$ h^{-1}	0.07	—	0.66
	$-OCH_2CF_2CF_2CF_2CHF_2$	99	37	98
	TON	128 000	37 000	98 000
	TOF $\times 10^6$ h^{-1}	0.26	0.07	0.20
Et_3SiH	$-C_5H_{11}$	6	6	42
	TON	—	—	66 000
	TOF $\times 10^6$ h^{-1}	—	—	0.13
	$-OCH_2CHOCH_2$	7	0	18
	TON	—	—	49 000
	TOF $\times 10^6$ h^{-1}	—	—	0.10
	$-OCH_2CF_2CF_2CF_2CHF_2$	62	0	53
	TON	95 000	—	53 000
	TOF $\times 10^6$ h^{-1}	0.19	—	0.11
TriEOS	$-C_5H_{11}$	91	24	99
	TON	308 000	24 000	307 000
	TOF $\times 10^6$ h^{-1}	0.61	0.05	0.61
	$-OCH_2CHOCH_2$	99	—	54
	TON	116 000	—	86 000
	TOF $\times 10^6$ h^{-1}	0.23	—	0.17
	$-OCH_2CF_2CF_2CF_2CHF_2$	99	0	93
	TON	129 000	—	147 000
	TOF $\times 10^6$ h^{-1}	0.26	—	0.30

not leached and could be reused in subsequent catalytic cycles. As the product is nonpolar, the polar liquid with the immobilized catalytically active phase is not washed out from the SILP surface. The hydrosilylation reactions with the use of triethylsilane are very slow and difficult to run, often their course is compared to that of the reaction with triphenylsilane in which the access to the Si–H bond is spatially hindered by phenyl groups. Triethylsilane contains electron-donating substituents and shows poor ability to form Si–C bonds, because of very low effectiveness of hydrogen atom transfer from Si–H bond to the carbon atom in the olefin double bond.

In view of the observed loss of catalytic abilities of SILP materials in subsequent catalytic cycles, selected samples of the post-reaction mixture was subjected to ICP analysis. The amounts of platinum and rhodium in these samples were below the level of detection (1 ppm). Taking into account our eelier experience with catalytic systems containing ionic liquids, we also checked the leaching of ionic liquids from the SILP systems studied. The sample of Pt-SILP with phosphonic ionic liquid $[P_{44414}][MeSO_4]$ was analyzed by ^{31}P NMR to assess the content of the liquid in the first and fifth catalytic cycle. The presence of the ionic liquid in the SILP samples after the first and the fifth catalytic cycle was confirmed, but its content in the reaction mixture was insignificant. Of course, slow leaching of the ionic liquid may have some insignificant effect on the catalytic activity of the SILP systems, but the majority of them maintained their activity up to at least 10 cycles and the most active ones – up to 15 subsequent cycles.

Materials and methods

Detail information on the analytical methods applied and the materials used in the studies reported is given in the ESI.†

Conclusions

Twenty four new SILP systems were obtained, supported on the oxide system TiO_2–SiO_2 and its combination with lignin (organic polymer). The structures, morphologies and physicochemical properties of the supports and the SILP systems were fully characterized. The determined adsorption parameters and thermal stability of the supports were proved to depend on the ratio of silicon and titanium precursors used in the sol–gel synthesis of the supports. The effectiveness of impregnation of the supports (TiO_2–SiO_2 or TiO_2–SiO_2/lignin) surfaces with the ionic liquids and immobilization of the catalytically active phase (homogeneous platinum or rhodium complexes) was verified by elemental analysis, SEM-EDX, IR and BET methods. According to the thermogravimetric analysis results, all obtained SILP systems were thermally stable at a temperature significantly higher than the hydrosilylation reaction temperature. All SILP systems obtained and studied in this work were catalytically active in hydrosilylation of 1-octene with 1,1,1,3,5,5,5-heptamethyltrisiloxane. The catalytically active materials were proved to be easy to isolate, so that they could be reused, and have been shown to be active in subsequent catalytic cycles. The Pt-SILP systems were found to more active than the systems with rhodium complexes, which was interpreted as a result of the more ionic character of the complex $[Pt(cod)Cl_2]$. From among the Pt-SILP materials, the highest catalytic activity was observed for those containing phosphonium and sulfonic ionic liquids and among the Rh-SILP materials, those with pyridinium ionic liquids. The SILP systems with the $[Ntf_2]^-$ anion were found to be more stable and in the reaction with their presence the Si–H conversion was higher than that in the systems with $[MeSO_4]^-$. FT-IR *in situ* results revealed that the activation time of the Pt-SILP systems is much more shorter than the corresponding time for the Rh-SILP materials. The reactions run with reagents of polar and nonpolar character revealed that the obtained SILP systems showed the highest catalytic activity and stability in the systems leading to products of nonpolar character. The polar reaction products lead to leaching of the ionic liquid together with the metal complex, thus to reduced activity or even inactivity in subsequent catalytic cycles. Taking into account the ease of synthesis of the SILP catalytic materials, their activity and possibility of reuse in subsequent catalytical cycles, they seem to make excellent alternatives to the homogeneous catalysts used in the reaction of hydrosilylation. The use of such materials could solve the problems with mass transport between the phases in standard two-phase systems and help reduce the cost related to the use of transition metal complexes.

Author contributions

Conceptualization, methodology, investigation, writing and editing original draft, project administration – *Olga Bartlewicz*; formal analysis, editing of original draft – *Mariusz Pietrowski*; investigation – *Marta Kaczmarek*; supervision, editing of original draft – *Hieronim Maciejewski*.

Conflicts of interest

There are no conflicts to declare.

Acknowledgements

This work was supported by grant Preludium no. UMO-2019/35/N/ST4/00494 financed by the National Science Centre Poland.

References

1 H. Maciejewski, K. Szubert and B. Marciniec, *Catal. Commun.*, 2012, **24**, 1–4.
2 B. Marciniec, H. Maciejewski, C. Pietraszuk and P. Pawluć, *Hydrosilylation. Comprehensive Review on Recent Advances*, Springer, 2009.
3 Y. Nakajima and S. Shimada, *RSC Adv.*, 2015, **5**, 20603–20616.
4 Z. Rappoport and Y. Apeloig, *The Chemistry of Organic Silicon Compounds*, Wiley, 2001.
5 R. G. Jones, W. Ando and J. Chojnowski, *Silicon-Containing Polymers*, Kluwer Acad. Press, 2000.

6 W. Zieliński, R. Kukawka, H. Maciejewski and M. Śmiglak, *Molecules*, 2016, **21**, 1115–1125.
7 M. Jankowska-Wajda, R. Kukawka, M. Śmiglak and H. Maciejewski, *New J. Chem.*, 2018, **42**, 5229–5236.
8 Y. Naganawa, Y. Maegawa, H. Guo, S. S. Gholap, S. Tanaka, K. Sato, S. Inagaki and Y. Nakajima, *Dalton Trans.*, 2019, **48**, 5534–5540.
9 O. Bartlewicz, I. Dąbek, A. Szymańska and H. Maciejewski, *Catalysts*, 2020, **10**, 1227–1246.
10 C. P. Mehnert and R. A. Cook, *J. Am. Chem. Soc.*, 2002, **124**, 12932–12933.
11 R. Fehrmann, A. Riisager and M. Haumann, *Supported Ionic Liquids. Fundamental and Applications*, Wiley-VCH, Weinheim, 2014.
12 J. M. Marinkovic, A. Riisager, R. Franke, P. Wasserscheid and M. Haumann, *Ind. Eng. Chem. Res.*, 2019, **58**, 2409–2420.
13 J. Brunig, Z. Csendes, S. Weber, N. Gorgas, R. Bittner, W. Limbeck, K. Bica, H. Hoffmann and K. Kirchner, *ACS Catal.*, 2018, **8**, 1048–1051.
14 F. Giacalone and M. Gruttadauria, *ChemCatChem*, 2016, **8**(4), 664–684.
15 B. V. Romanovsky and I. G. Tarhanov, *Russ. Chem. Rev.*, 2017, **86**, 444–458.
16 S. More, S. Jadhav, R. Salunkhe and A. Kumbhar, *Mol. Catal.*, 2017, **442**, 126–132.
17 J. Brunig, Z. Csendes, S. Weber, N. Gorgas, R. W. Bittner, A. Limbeck, K. Bica, H. Hoffmann and K. Kirchner, *ACS Catal.*, 2018, **8**, 1048–1051.
18 R. Castro-Amoedo, Z. Csendes, J. Brunig, M. Sauer, A. Foelske-Schmitz, N. Yigit, G. Rupprechter, T. Gupta, A. M. Martins, K. Bica, H. Hoffmann and K. Krichner, *Catal. Sci. Technol.*, 2018, **8**, 4812–4820.
19 L. L. Hench and J. K. West, *Chem. Rev.*, 1990, **90**, 33–72.
20 U. G. Akpan and B. H. Hameed, *Appl. Catal., A*, 2010, **375**, 1–11.
21 G. Wypych, *Handbook of Fillers*, ChemTec Publishing, Toronto, 2nd edn, 1999.
22 X. Chen and S. S. Mao, *Chem. Rev.*, 2007, **107**, 2891–2959.
23 O. Ola and M. M. Maroto-Valer, *J. Photochem. Photobiol., C*, 2015, **24**, 16–42.
24 S. F. A. Taliba, W. H. Azmib, I. Zakariaa, W. A. N. W. Mohameda, A. M. I. Mamata, H. Ismaila and W. R. W. Daud, *Energy Procedia*, 2015, **79**, 366–371.
25 R. Q. Zhang and W. J. Fan, *J. Cluster Sci.*, 2006, **17**, 541–563.
26 K. Siwińska-Stefańska, O. Bartlewicz, P. Bartczak, A. Piasecki and T. Jesionowski, *Adsorption*, 2019, **25**, 485–499.
27 M. Cozzolino, M. Di Serio, R. Tesser and E. Santacesaria, *Appl. Catal., A*, 2007, **325**(2), 256–262.
28 G. Mul, A. Zwijnenburg, B. van der Linden, M. Makkee and J. A. Moulijn, *J. Catal.*, 2001, **201**, 128–137.
29 Ł. Klapiszewski, K. Siwińska-Stefańska and D. Kołdyńska, *Chem. Eng. J.*, 2017, **314**, 169–181.
30 Ł. Klapiszewski, J. Zdarta and T. Jesionowski, *Colloids Surf., B*, 2018, **162**, 90–97.
31 B. Marciniec, K. Szubert, M. J. Potrzebowski, I. Kownacki and H. Maciejewski, *ChemCatChem*, 2009, **1**, 304–310.
32 M. Jankowska-Wajda, O. Bartlewicz, A. Walczak, A. R. Stefankiewicz and H. Maciejewski, *J. Catal.*, 2019, **374**, 266–275.
33 R. Kukawka, A. Pawłowska-Zygarowicz, R. Januszewski, J. Działkowska, M. Pietrowski, M. Zieliński, H. Maciejewski and M. Śmiglak, *Catalysts*, 2020, **10**, 1414–1425.
34 A. Kołodziejczak-Radzimska, J. Zdarta, F. Ciesielczyk and T. Jesionowski, *Korean J. Chem. Eng.*, 2018, **35**, 2220–2231.
35 O. Bartlewicz, M. Zieliński, M. Kaczmarek and H. Maciejewski, *Mol. Catal.*, 2021, **509**, 111615–111624.
36 T. Jesionowski, Ł. Klapiszewski and G. Milczarek, *J. Mater. Sci.*, 2014, **49**, 1376–1385.
37 R. Kukawka, A. Pawlowska-Zygarowicz, J. Dzialkowska, M. Pietrowski, H. Maciejewski, K. Bica and M. Smiglak, *ACS Sustainable Chem. Eng.*, 2019, **7**, 4699–4706.
38 A. L. Linsebigler, G. Lu and J. Yates, *Chem. Rev.*, 1995, **95**, 735–758.
39 D. Kondarides, *Photocatalysis, Encyclopedia of Life Support Systems*, Oxford, 2010.
40 M. Thommes, K. Kaneko, A. V. Neimark, J. P. Olivier, F. Rodriguez-Reinoso, J. Rouquerol and K. S. W. Sing, *Pure Appl. Chem.*, 2015, **87**, 1051–1069.
41 G. E. Berendsen and L. de Golan, *J. Liq. Chromatogr. Relat. Technol.*, 1978, **1**(5), 561–586.
42 V. Calo, A. Nacci and A. Monopoli, *Eur. J. Org. Chem.*, 2006, 3791–3802.
43 S. Subbiah, V. Srinivasadesikan, M.-C. Tseng and Y.-H. Chu, *Molecules*, 2009, **14**, 3780–3813.